Ecological Processes

RESEARCH

Open Access

Comparing leaf area index estimates in a Mediterranean forest using field measurements, Landsat 8, and Sentinel-2 data

Alessandro Sebastiani[1,2*], Riccardo Salvati[3] and Fausto Manes[4]

Abstract

Background Leaf area index (LAI) is a key indicator for the assessment of the canopy's processes such as net primary production and evapotranspiration. For this reason, the LAI is often used as a key input parameter in ecosystem services' modeling, which is emerging as a critical tool for steering upcoming urban reforestation strategies. However, LAI field measures are extremely time-consuming and require remarkable economic and human resources. In this context, spectral indices computed using high-resolution multispectral satellite imagery like Sentinel-2 and Landsat 8, may represent a feasible and economic solution for estimating the LAI at the city scale. Nonetheless, as far as we know, only a few studies have assessed the potential of Sentinel-2 and Landsat 8 data doing so in Mediterranean forest ecosystems. To fill such a gap, we assessed the performance of 10 spectral indices derived from Sentinel-2 and Landsat 8 data in estimating the LAI, using field measurements collected with the LI-COR LAI 2200c as a reference. We hypothesized that Sentinel-2 data, owing to their finer spatial and spectral resolution, perform better in estimating vegetation's structural parameters compared to Landsat 8.

Results We found that Landsat 8-derived models have, on average, a slightly better performance, with the best model (the one based on NDVI) showing an R^2 of 0.55 and NRMSE of 14.74%, compared to R^2 of 0.52 and NRMSE of 15.15% showed by the best Sentinel-2 model, which is based on the NBR. All models were affected by spectrum saturation for high LAI values (e.g., above 5).

Conclusion In Mediterranean ecosystems, Sentinel-2 and Landsat 8 data produce moderately accurate LAI estimates during the peak of the growing season. Therefore, the uncertainty introduced using satellite-derived LAI in ecosystem services' assessments should be systematically accounted for.

Keywords Mediterranean forest, Leaf area index, Field measurement, Multispectral satellite imagery, Sentinel-2, Landsat 8, Spectral vegetation index, Global change

*Correspondence:
Alessandro Sebastiani
alessandro.sebastiani@cnr.it
Full list of author information is available at the end of the article

Background

The influence of ecosystem services (ESs) on human psychophysical well-being is nowadays largely acknowledged (Kosanic and Petzold 2020; Leviston et al. 2018). Urban green areas such as urban and peri-urban forests provide space for social interactions (Enssle and Kabisch 2020), cleaner air (Manes et al. 2012, 2014, 2016; Muresan et al. 2022; Nardella et al. 2023), mitigation of the extreme summer temperatures (Marando et al. 2019), flood prevention (Farrugia et al. 2013; Sebastiani and Fares 2023), and cultural opportunities (Lausi et al. 2022). Hence, ESs generate a remarkable monetary value, estimated at $ 125 trillion/year (Costanza et al. 2014) by, among others, preventing hospitalization for respiratory diseases, avoiding extreme floods in urban areas (Vázquez-González et al. 2019), and reducing the health impact of heatwaves (Sebastiani et al. 2021a). Indeed, the exposure of citizens to greenness is directly associated with positive health outcomes (Manes et al. 2012; Orioli et al. 2019).

The EU has recognized the role and value of ESs in urban environments. The New EU Forest Strategy for 2030 (EC 2020a, b) highlights the need for re- and afforestation and tree planting in urban and peri-urban areas as a winning strategy to mitigate climate change and environmental risks, create job opportunities and enhance people's physical and mental health. For this reason, the EU pledged to plant at least 3 billion trees by 2030 and, in the EU Biodiversity Strategy for 2030 (EC 2020a; b), has called on cities with at least 20,000 inhabitants to develop an ambitious greening strategy, to provide accessible green spaces for city dwellers and improve the connections between existing green areas. The proposed Nature Restoration law (EC 2022) advocates for the no-net loss of urban green areas by 2030 as well as the enhancement of urban green spaces. The Italian Government is also pushing for planting more trees by allocating 300 million EUR of the National Recovery and Resilience Plan (PNRR) for urban forestry interventions to be implemented over the next few years. Hence, in the upcoming years, properly addressing the creation and management of urban and peri-urban green areas, also accounting for the ESs' delivery (Blasi et al. 2017), will be critical to establishing social and spatial justice in cities (Langemeyer and Connolly 2020).

In this framework, the leaf area index (LAI), defined as the one-sided green leaf area per unit ground area (Robinson and Lundholm 2012), is a key indicator for the assessment of canopies processes such as net primary production and evapotranspiration (Bréda 2008). As such, the LAI is often used as a key input parameter for modeling regulating ESs such as air pollutants removal (Nowak et al. 1998; Manes et al. 2016; Sebastiani et al. 2021b), mitigation of the urban heat island effect (Xiao et al. 2018), and water runoff (Tesemma et al. 2015).

LAI field measures are extremely time-consuming and require remarkable economic and human resources; consequently, these are generally carried out for small areas such as tree lines, urban parks, or small forest patches. A multitude of studies used satellite-derived products, which are in several cases delivered for free and in near-real-time (Fuster et al. 2020; Jiang et al. 2010; Manes et al. 1997a; Viña et al. 2011), for the estimation of LAI. Currently, several satellite-derived LAI products such as MODIS and Copernicus Global Land Service have been consistently validated all around the world for different periods of the year, showing appreciable accuracies (Fuster et al. 2020; Serbin et al. 2013; Yan et al. 2016). However, the spatial resolution of those products is included between 500 and 300 m and may not be suitable for studies at the fine scale, e.g., at the city level, therefore providing a limited contribution to upcoming urban planning strategies.

In this context, spectral indices (SIs) computed using high-resolution multispectral satellite imagery like Sentinel-2 and Landsat-8, may represent a feasible, economic solution for estimating the LAI at a finer scale (Dong et al. 2020; Meyer et al. 2019). Nonetheless, as far as we know, only a few studies have assessed the potential of Sentinel-2 and Landsat 8 data in estimating the LAI in Mediterranean forest ecosystems (Chrysafis et al. 2020).

In this study, we compared the performance of Sentinel-2 and Landsat 8 data in estimating the LAI. Specifically, we expected Sentinel-2 data to be more accurate and precise, as they come up with a better spatial and spectral resolution. Accordingly, we tested the performance of 10 SIs derived from Sentinel-2 and Landsat 8 data in predicting the LAI. We used field measurements collected with the LI-COR LAI 2200c as a reference and performed a linear regression between the field-measured LAI and each one of the SIs.

Methods

Study area

The Presidential Estate of Castelporziano (PECp) is a State natural reserve of 6,000 hectares almost entirely covered by natural forests (Conte et al. 2022; Manes et al. 2021); it is located about 20 km southwest of the center of Rome (Central Italy), laying along the coast (Fig. 1). The climate is Mediterranean, with average monthly summer and winter temperatures reaching 25 °C and 6–12 °C, respectively; mean annual precipitation is 740 mm, with a marked period of summer aridity (Manes et al. 1997b; Seufert et al. 1997).

The PECp hosts a remarkable functional and structural biodiversity, with forest stands of different functional

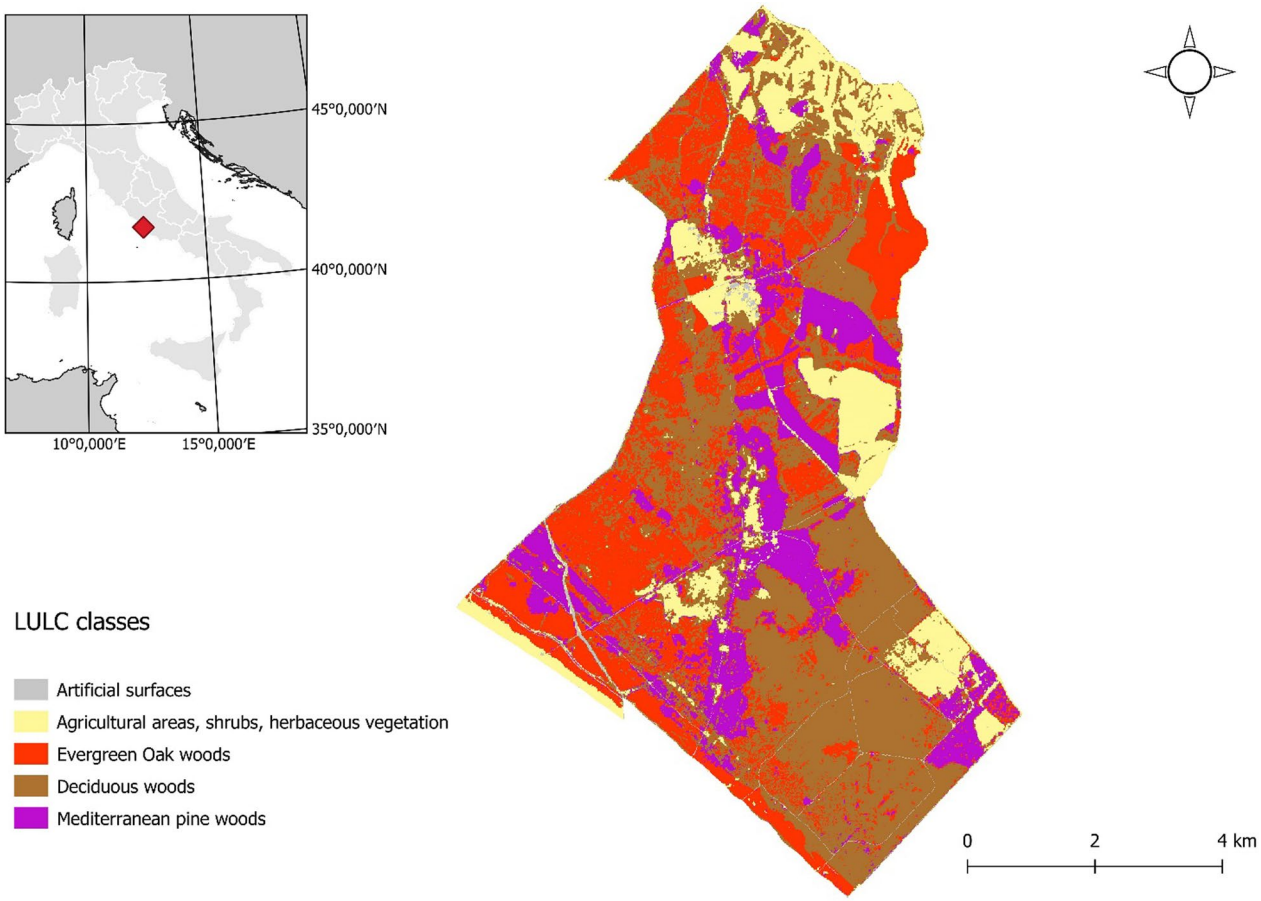

Fig. 1 Land use and land cover map of the PECp, derived from the supervised classification of Sentinel-2 data

groups (FGs) of vegetation including evergreen broadleaves (e.g., *Quercus ilex, Quercus suber* dominant), deciduous broadleaves (*Q. frainetto, Q. cerris* dominant), conifers (*Pinus pinea* plantations) and Mediterranean maquis (Manes et al. 1997b). The PECp is also a hotspot of faunal biodiversity, hosting more than 2900 animal species (Castracani et al. 2010), including about 300 macroinvertebrates' taxa (Bazzanti 2015). For this reason, it falls within the Natura2000 network (site IT6030084) as both a Special Protection Area and a Special Area of Conservation.

Drought stress assessment

The study area is usually subject to prolonged drought periods in summer when high temperatures and low precipitations occur; however, the vegetation is well-adapted to such conditions, as it developed multiple adaptative strategies for controlling the water loss (Manes et al. 1997c, d).

A prolonged or extremely intense summer drought might alter the plant's ecophysiological processes such as transpiration and photosynthesis (Hoff and Rambal 2003; Galmés et al. 2007). Drought would hence lower the leaves' water and chlorophyll content, which heavily shapes the canopy's reflectance detected by remote sensors and, consequently, vegetation SIs (Deshayes et al. 2006). Moreover, drought-tolerant species are characterized by low specific leaf area, which affects the extension of the leaves' surface (Waring et al. 1991) and, consequently, their light-blocking effect. For this reason, drought may also affect the field measurement of LAI.

Therefore, it is crucial to account for the eventual drought stress that may have occurred during the field campaign, as it might provide a valuable key for properly interpreting the results.

For this reason, we provide insight into any possible drought stress by:

i) Comparing the historical (1981–2020) and the annual (2021) Walter–Lieth diagrams, derived by elaborating the climatological records of the PECp in the Climatol package implemented in Rstudio (Guijarro 2019).

ii) Computing the Normalized Difference Moisture Index (NDMI) derived from Sentinel-2 data for the months of June, July, and August 2021. NDMI uses NIR and SWIR bands and varies according to the moisture levels of vegetation; values above 0.2 indicate low water stress for high canopy areas (EOS data analytics 2022).

Field campaign for the LAI measurement

The field campaign was conducted in the first week of July 2021 for 5 consecutive days. We used LI-COR LAI-2200c Plant Canopy Analyzer to perform non-destructive LAI measures. The instrument is equipped with a fisheye lens and detects light interception in five concentric sky sectors (Cutini et al. 1998); LAI is computed by comparing the diffuse radiation underneath the canopy to measures taken in large clearings with no light-blocking objects (Breda 2003; Danner et al. 2015).

Following the recommendations by LI-COR, we used the single sensor, scattering correction procedure, which is required for direct sunlight conditions. Measures were taken with a 270° cap, which allowed for removing the light-blocking effect of the operator and other objects (i.e., branches); each measure was georeferenced with the built-in GPS. Raw data were then transferred and elaborated in FV220, the dedicated software freely delivered by LI-COR. In post-processing, for each measure, we excluded rings with inconsistent values, which may be caused by factors such as light blocking by branches and slope. According to the LAI 2200c user manual (LI-COR Biosciences 2013), we excluded measures with an HDOP (Horizontal Dilution of Precision, a measure indicating the precision of the GPS positioning) higher than 5, to minimize the effect of positioning errors.

We did not account for the vegetation under the measuring height, which has been hypothesized to influence the field LAI measurement (Meyer et al. 2019); in fact, the forests' understory was sparse, and never dense enough to hinder the walk below the canopy.

Besides drought stress, biotic stress was also critical for the field campaign. In fact, since 2018, pine stands of the PECp have been infested by *Toumeyella parvicornis*, a pest known for causing a reduction in shoot development, yellowing and desiccation of the needles, and lack of vegetative renewal (Di Sora et al. 2022). For the sake of representativeness, we purposely avoided stands that showed visible yellowing and desiccation of the needles; however, it is noteworthy that, according to the unpublished data of the PECp, two pine stands (the upper right and the central, please refer to Fig. 2) were likely infested by *T. parvicornis* from 2020 onwards.

We collected 193 LAI measures (Fig. 2) divided as follows for the different FGs of vegetation: deciduous broadleaves (88 measures), evergreen broadleaves (53 measures), and conifers (52 measures). Measures were taken at a distance of at least 10 m from each other; each measure was made by four readings, spaced about 1 m along a linear transect.

Satellite data acquisition and processing

We used Sentinel-2 and Landsat 8 data, which have a spatial resolution included between 10 and 30 m, to compute several SIs (Table 1), that were subsequently used as predictors for the estimation of the field-measured LAI. SIs are somehow related to the chlorophyll content of vegetation and are therefore widely used to evaluate its health conditions (Peng and Gitelson 2011); plus, these can be easily retrieved in multitemporal series over large areas, with minimum economic effort.

A Sentinel-2 image, acquired on the 4th of July 2021 was downloaded from the Copernicus Open Access Hub. Sentinel-2 images are made of 13 spectral bands, including 3 bands known as the red-edge bands (Clevers and Gitelson 2013); the red edge is a spectral region between red and near-infrared, in which the reflectance curve of vegetation rapidly changes, shifting from high absorption to high reflectance (Sun et al. 2020). Because of that, Sentinel-2 red-edge bands are massively used for vegetation monitoring. Except for band 1, which has a spatial resolution of 60 m, Sentinel-2 bands have a spatial resolution of 10–20 m. We used a 2A-level product, which provides Bottom-of-Atmosphere (BOA) reflectance and is systematically generated over Europe. Elaborations were conducted using the Sentinel Application Platform (SNAP) software, freely delivered by the European Space Agency; to compute the SIs, we used both the biophysical processor and the band calculator (Djamai and Fernandes 2018; Louis et al. 2016). In this study, we computed four Sentinel-2 derived indices (Table 1), which are LAI, Normalized Difference Vegetation Index (NDVI), Normalize Difference Water Index (NDWI), and Normalize Burned Ration (NBR). All the Sentinel-2-derived SIs have a spatial resolution of 10 m except for the NBR, which has a spatial resolution of 20 m. In addition, to fully exploit the potential of Sentinel-2 data, the following simple band ratios (SRs) were computed: SR56 (band 5/ band 6); SR57 (band 5/ band 7); SR67 (band 6/ band 7). Band 5, 6 and 7 (spatial resolution of 20 m for each one) were chosen as these fall in the so-called red edge region.

A Level 1 Landsat 8 image, acquired on the 8th of July 2021, was downloaded from the USGS website. The processing operations, including conversion to reflectance and atmospheric correction, were executed using the Semi-Automatic Classification Plugin (Congedo 2016)

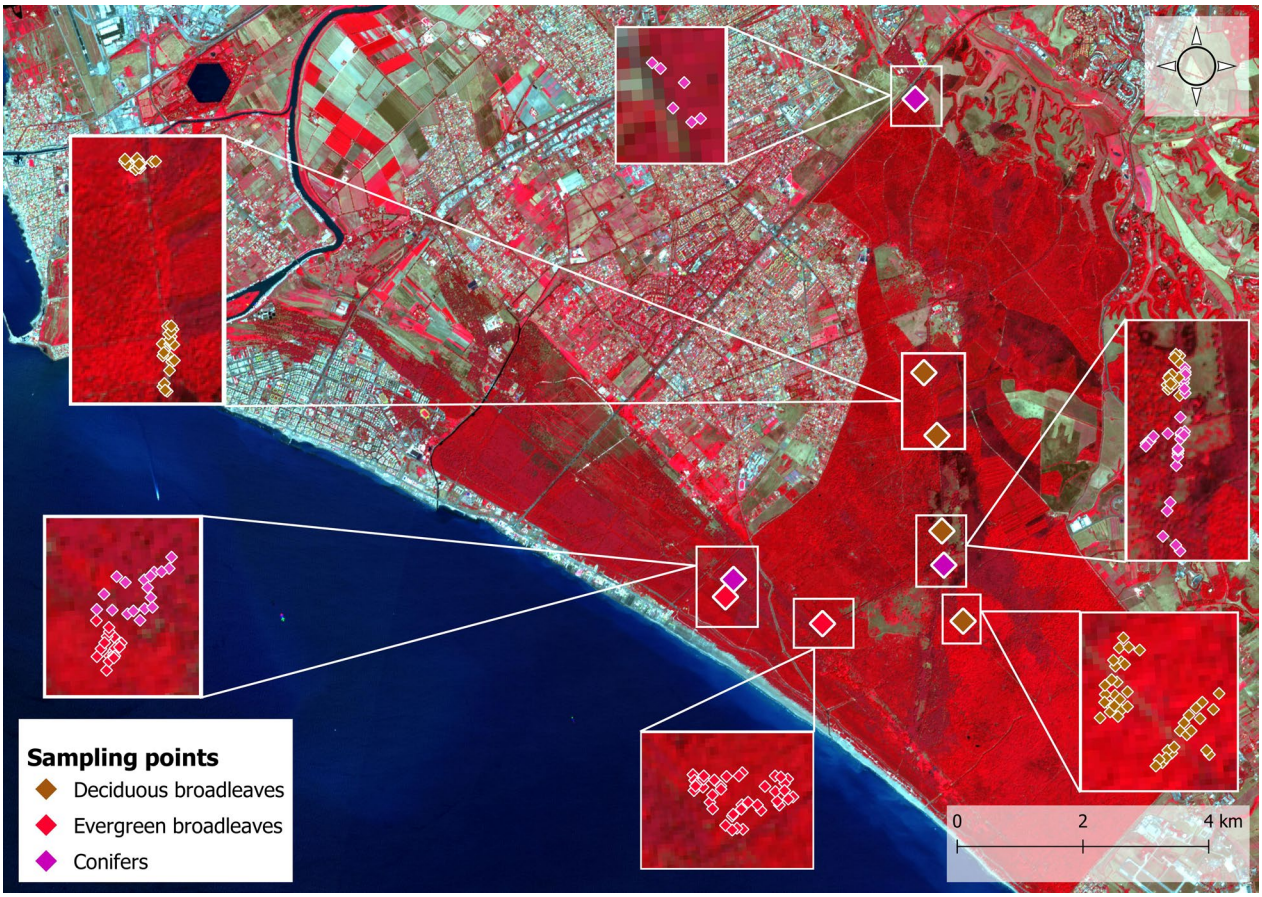

Fig. 2 Sampling points of the field campaign for LAI measurement. The background image is a false-color infrared derived from Sentinel-2 data

Table 1 Overview of the spectral indices considered for the present work

Platform	Index	Formula	Spatial resolution (m)
Sentinel-2	LAI	SNAP biophysical processor	10
	NDVI	$\frac{B8-B4}{B8+B4}$	10
	NDWI	$\frac{B3-B8}{B3+B8}$	10
	NBR	$\frac{B8a-B12}{B8a+B12}$	20
	SR56	$\frac{B5}{B6}$	20
	SR57	$\frac{B5}{B7}$	20
	SR67	$\frac{B6}{B7}$	20
Landsat 8	NDVI	$\frac{B4-B5}{B4+B5}$	30
	NDWI	$\frac{B3-B5}{B3+B5}$	30
	NBR	$\frac{B5-B7}{B5+B7}$	30

implemented in QGIS. We computed 3 spectral indices (Table 1), which are, NDVI, NBR, and NDWI; the Landsat 8-derived SIs have a spatial resolution of 30 m.

Statistical analysis

First, we calculated Spearman's correlation coefficient and the associated *p*-value between the field-measured LAI and the selected spectral indices, to provide a preliminary quantification of their degree of association.

Then, we performed a single linear regression to build predictive models, using each of the SIs as a predictor for the field-measured LAI.

Descriptive statistics of the field-measured and estimated LAI were computed, to provide a comprehensive overview of the canopy's condition at the measurement's time.

The performance of each model was assessed by computing the root mean square error (RMSE), that is, a metric for estimating how the estimated LAI values are concentrated around the best-fitting line. The RMSE was calculated using the following equation:

$$\mathrm{RMSE} = \sqrt{\frac{\sum_{i=1}^{n}\left(y_i - \hat{y}_i\right)^2}{n}}, \quad (1)$$

where y_i is the observed value, $\hat{y}_i$ the predicted value, and n is the number of observations.

RMSE was computed using the leave-one-out-cross-validation (LOOCV) technique, using the caret package implemented in RStudio (Kuhn et al. 2022). This approach is frequently used with small input datasets (Wong 2015), and consists of training the model on all observations except one, which is used to test the set. This procedure is repeated for all observations; to estimate the overall predictive performance of the model, the predictive scores for each of the test sets are eventually summed (Gronau and Wagenmakers 2019).

We also computed the Normalized RMSE (NRMSE), applying the following equation:

$$\mathrm{NRMSE} = \frac{\mathrm{RMSE}}{y_{\max} - y_{\min}} \times 100, \quad (2)$$

where $y_{\max}$ and $y_{\min}$ are the maximum and minimum field-measured LAI values, respectively.

Results and discussion

Figure 3 shows the historical (1981–2020) and annual (2021) Walter–Lieth (Bagnouls 1953; Reader et al. 1974) diagram for the PECp. The summer drought of 2021 was longer and more intense compared to the usual, as it lasted from May to October. Even though such a prolonged drought period has likely affected the vegetation's condition in the long run, no visible sign of drought stress such as defoliation or leaves yellowing was found on trees at the measurement time. Evergreen broadleaves of the PECp have already proved to be extremely tolerant to water stress by adopting a "water saving strategy" (Anselmi et al. 2004; Manes et al. 1997a), whereas *P. pinea* stands are generally more sensitive (Manes et al. 1997c). It is also noteworthy that the NDMI did not drop drastically in July for both deciduous and evergreen broadleaves, whereas it was very low for conifers throughout the summer (Table 2). Therefore, we can exclude that deciduous and evergreen broadleaf were affected by drought stress at the measurement time, whereas conifers were somehow in a water shortage. We argue that this may be due to the atypically abundant precipitation, that occurred during March and April, which

Table 2 NDMI for each functional group (FG) of vegetation during the summer of 2021

FG	Date		
	June 14	July 7	August 18
Deciduous broadleaves	0.31	0.28	0.23
Evergreen broadleaves	0.36	0.33	0.27
Conifers	0.04	0.03	− 0.12

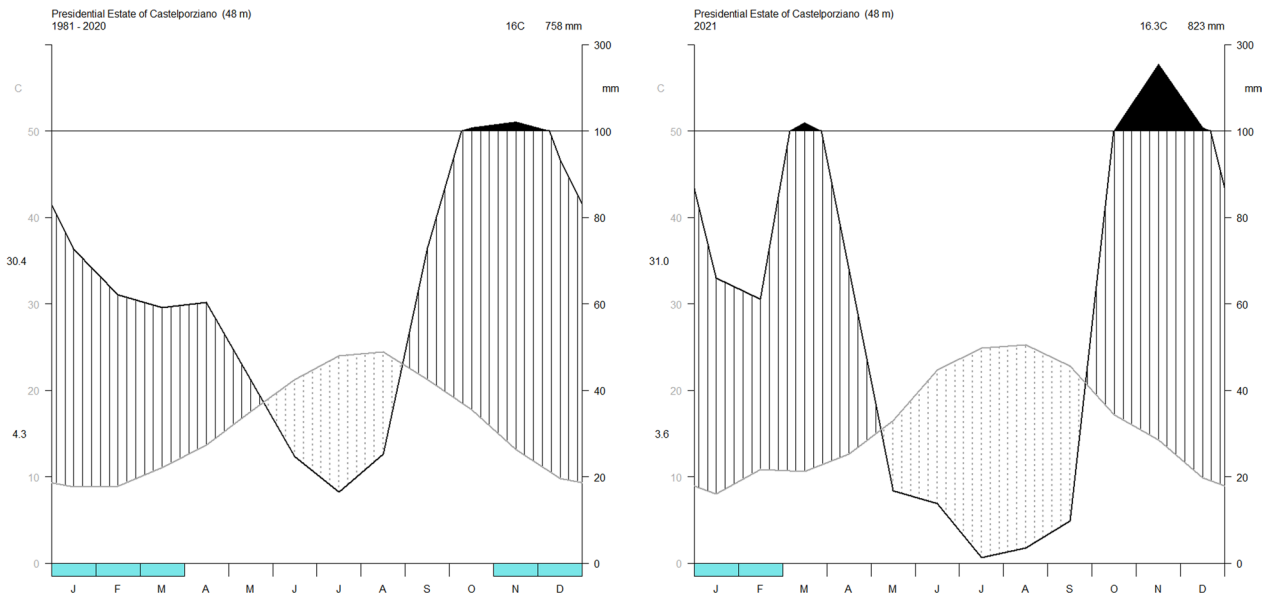

Fig. 3 Walter–Lieth diagram of the Presidential estate of Castelporziano for the period 1981–2020 (left) and for the year 2021 (right). Months are indicated by the letters at the bottom of the diagram. Temperature (°C) is represented on the left axis; precipitation (mm) is on the right axis. The blue blocks at the bottom of the graph indicate the probable frost months, when absolute monthly minimum temperatures are equal to or lower than 0

contributed to keeping acceptable levels of soil moisture during the first week of July.

Regarding the *T. parvicornis* infestation suffered by pine stands, despite the absence of marked visible signs on the sampled stands, it has likely affected SIs computation. In theory, it should be lowered by the detrimental effect of the pest, which reduces the pigment content of leaves, thus altering the canopy's reflectance. However, it is impossible to account for such an impact without a proper experimental design, and it might be better addressed in a dedicated study.

The boxplot for the field-measured LAI values is shown in Fig. 4A. Deciduous broadleaves and evergreen broadleaves display high median LAI values, between 4.5 and 4.9, whereas conifers' median LAI value is significantly lower, attested at 2.3. As expected, in all cases (Fig. 4B–K) the estimated LAI follows a similar pattern compared to the measured one, with conifers displaying lower LAI than deciduous and evergreen broadleaves. Interestingly, despite comparable median values, the interquartile range (IQR) of the estimated LAI is systematically lower than the one of the measured LAI, indicating that the values' distribution is more centered around the median. This happens for all the considered SIs and in each one of the FGs. The lower dispersion of the estimated LAI could be attributed to the pixel size: indeed, whereas a spot field measure ensures that the resulting LAI is fully attributable to one or a few trees, a window ranging from 10 m × 10 m to 30 m × 30 m might include several trees, which likely flatten the resulting LAI around a well-representative value.

Table 3 shows Spearman's correlation coefficient between the measured LAI and the selected SIs. The absolute correlation value ranges from 0.54 to 0.65, indicating a quite strong association between the considered variables; a high level of significance is reached. Interestingly, spectral indices are also strongly correlated with each other (Fig. 5), with correlation coefficients exceeding the absolute value of 0.5 in almost all cases. The Landsat 8-derived NDWI and the SRs are the only indices with a strong negative correlation with other indices (Fig. 5). Such a strong association is not surprising, as Sentinel-2 data are specifically designed to provide data continuity to the Landsat 8 mission (ESA 2023).

All models show comparable performances, with R^2 included between 0.46 and 0.55 and NRMSE ranging from 14.74% to 18.01%. Overall, our results are quite following what was found by Meyer et al. (2019), who found

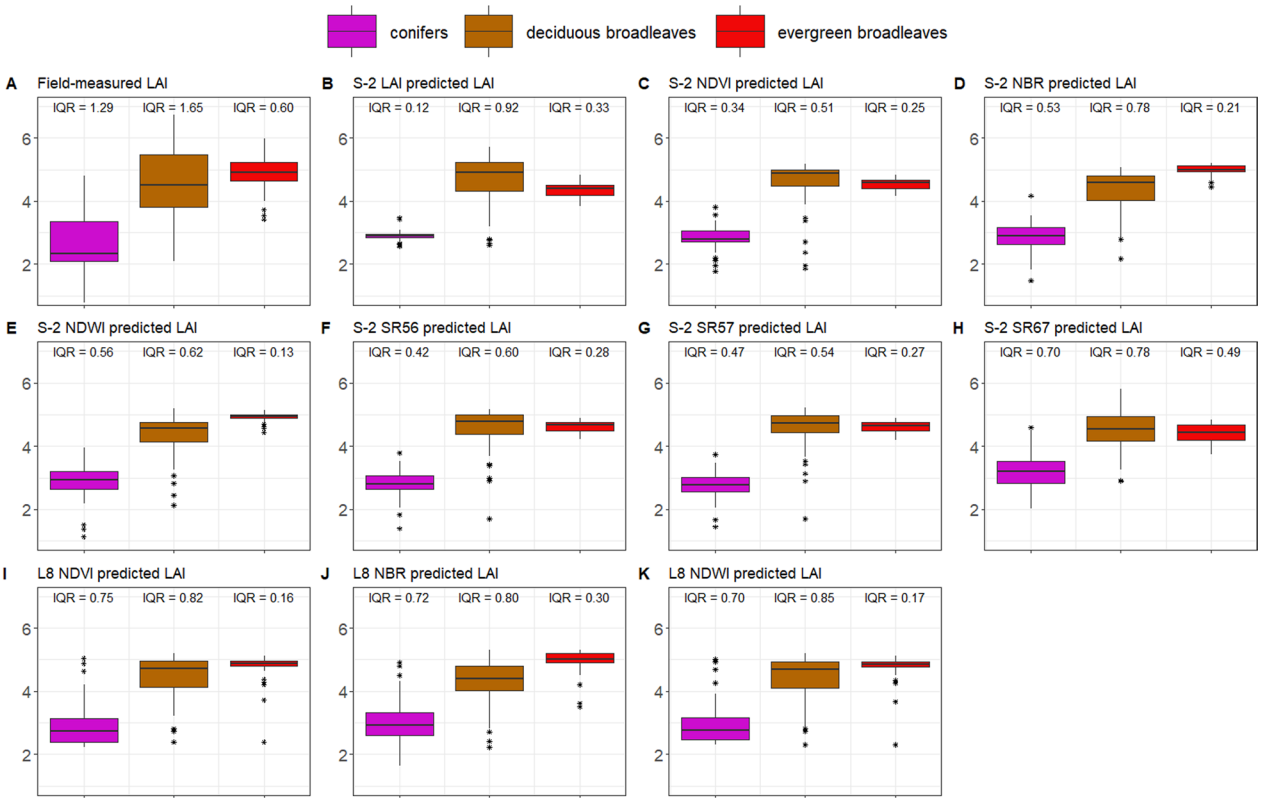

Fig. 4 Boxplot of the field-measured LAI and SI-predicted LAI for each functional group of vegetation. IQR on top of each group represents the interquartile range. The asterisks represent the outliers

Table 3 Spearman's correlation coefficients (and *p*-value) between the field-measured LAI e and the selected spectral indices

Index	Spearman
S-2 LAI	0.604*
S-2 NDVI	0.595*
S-2 NBR	0.595*
S-2 NDWI	0.601*
S-2 SR56	− 0.589*
S-2 SR57	− 0.596*
S2 SR67	− 0.541*
L8 NDVI	0.654*
L8 NBR	0.607*
L8 NDWI	− 0.634*

The asterisk represents a high level of significance, with *p*-value lower than 0.05

that Sentinel-2 and Landsat 8 had comparable performances in predicting the actual LAI values over boreal forests in Germany.

Among Sentinel-2 models, the NDWI and NBR-derived ones are the best performing, with R^2 above 0.50 and NRMSE at around 15%. As for SRs, SR56 and SR57 show moderate performances, comparable to other S-2-derived indices. Similar findings were reported by Meyer et al. (2019), who also found that red-edge indices do not outperform other indices in estimating the field-measured LAI. SR67 has instead a markedly worse performance compared to all the other SIs. This is quite far from what we expected, as red-edge bands are notorious for being extremely sensitive to vegetation's health status (Sun et al. 2020).

Landsat 8-derived models perform consistently better than Sentinel-2-derived ones, with R^2 attested between 0.52 and 0.55, and NRMSE between 14.74% and 15.15%. Overall, 10-m resolution models are systematically outperformed by coarser ones. Therefore, more in-depth studies aimed at understanding the mechanisms underpinning such findings are required. The results are summarized in Fig. 6 and Table 4.

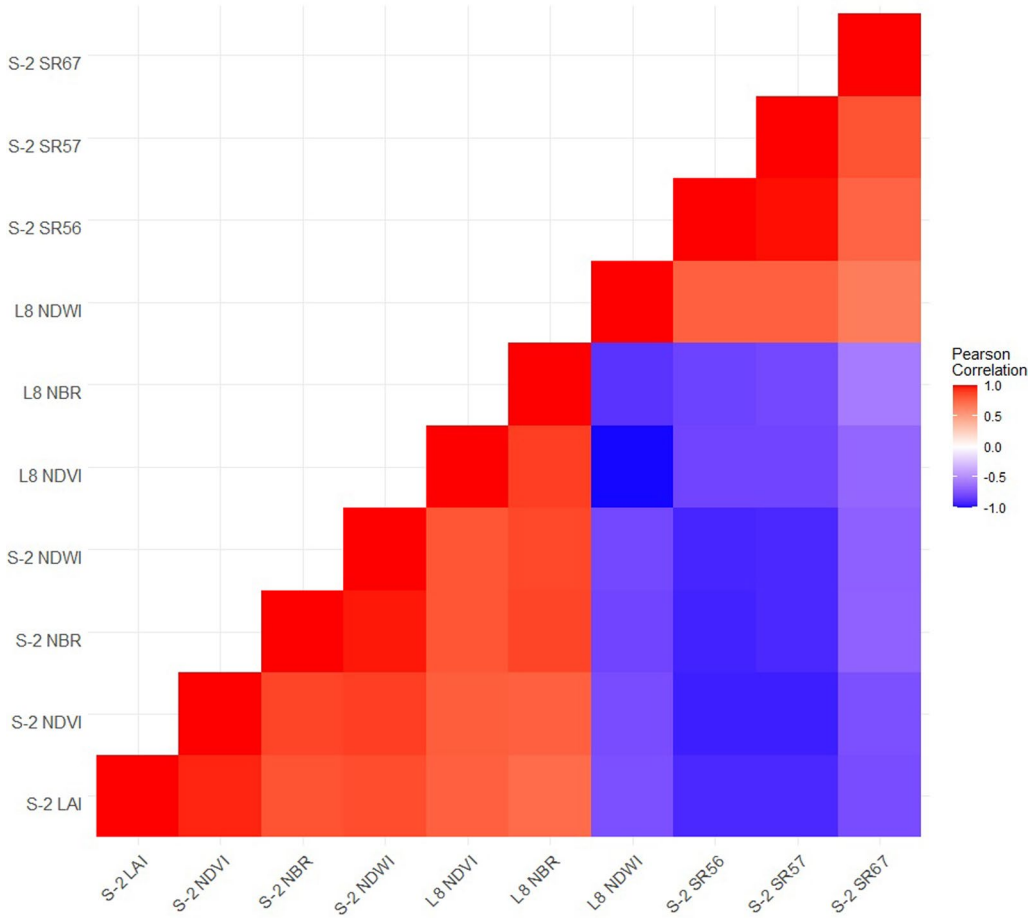

Fig. 5 Pairwise correlation matrix between the selected SIs

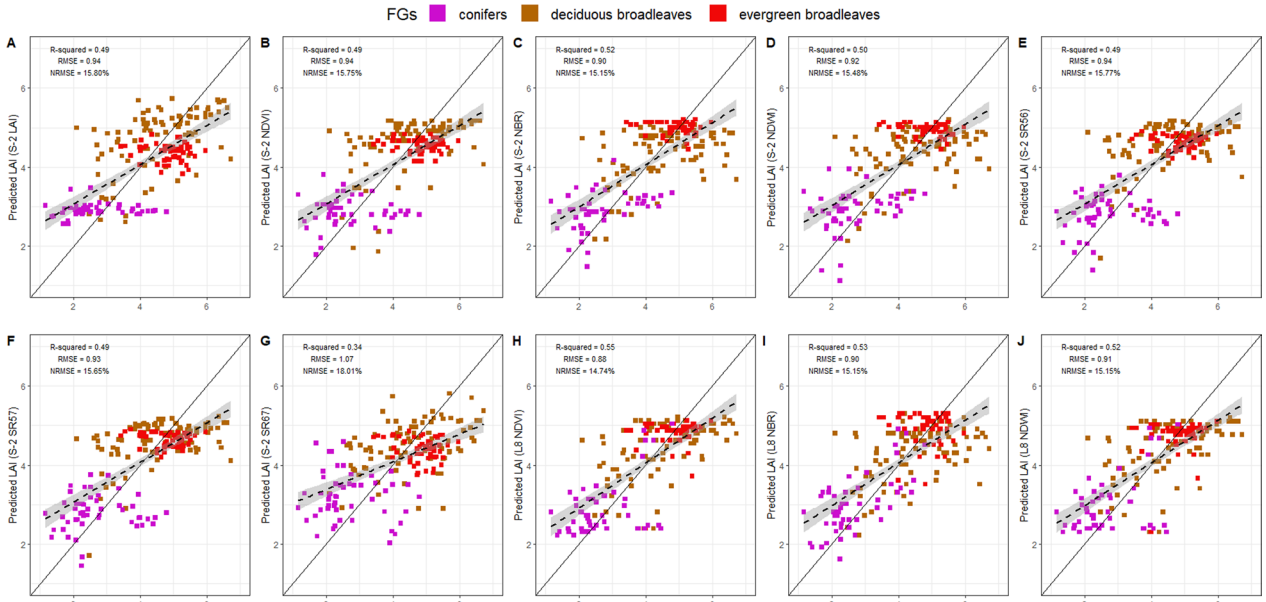

Fig. 6 Scatter plot of measured (*x*-axis) vs estimated (*y*-axis) LAI. The solid line is the 1:1 line, which represents the ideal fit. The dashed line is the actual regression line

Table 4 R-squared (R^2), root mean square error (RMSE), normalized root mean square error (NRMSE), mean absolute error (MAE), and the equation describing the relation

VI	R^2	RMSE	NRMSE (%)	MAE	Equation
S-2 LAI	0.49	0.94	15.80	0.79	$y = 1.917 + 1.005x$
S-2 NDVI	0.49	0.94	15.75	0.78	$y = -2.034 + 8.474x$
S-2 NBR	0.52	0.90	15.15	0.70	$y = 0.448 + 6.895x$
S-2 NDWI	0.50	0.92	15.48	0.72	$y = 0.940 + 6.260x$
S-2 SR56	0.49	0.94	15.77	0.77	$y = 7.714 - 8.861x$
S-2 SR57	0.49	0.93	15.65	0.78	$y = 7.174 - 9.176x$
S-2 SR67	0.34	1.07	18.01	0.89	$y = 19.110 - 18.440x$
L8 NDVI	0.55	0.88	14.74	0.70	$y = 1.564 + 8.281x$
L8 NBR	0.53	0.90	15.15	0.70	$y = -2.157 + 9.945x$
L8 NDWI	0.52	0.91	15.15	0.72	$y = 2.219 - 8.492x$

In the latter, *y* is the estimated LAI, and *x* is the considered VI

As stated by previous studies (Brown et al. 2021; Filipponi 2021; Pasqualotto et al. 2019), we also observed a general underestimation of the satellite-derived LAI compared to the field-measured one for high-measured LAI values, e.g., above 5 (Fig. 6). We argue that may be due to the methodological approaches for in situ and remote LAI estimation. Indeed, LI-COR LAI-2200 is affected by the presence of all light-blocking objects including branches and dead wood, which contribute to the computation of the LAI. As for remote-sensed spectral indices, these are instead computed based on the solar radiation reflected and absorbed by pigments of the mesophyll and are therefore exclusively related to the photosynthetic portion of the canopy. Plus, as observed in previous studies (Tesfaye and Awoke 2021; Zhou et al. 2017) SIs incur spectrum saturation, that is, they do not increase once that vegetation's reflectance overcomes a certain threshold. Saturation is more evident for areas with very dense vegetation, during the peak of the growing season (Gao 2000; Todd et al. 1998). We argue that this is also the case in our study: indeed, in both Sentinel-2 and Landsat 8-derived models, the estimated LAI reaches its limit at around 5, whereas field-measured LAI is on several occasions well above 6.

Therefore, according to our findings, the Sentinel-2 and Landsat 8 data are essentially equivalent in estimating the LAI. Landsat 8 performs slightly better; however, its coarser spatial resolution (30 m, compared to Sentinel's 10 m or 20 m) may not be suitable for some elements of the urban green infrastructure such as isolated street trees or tree lines, which in turn may have a critical role in upcoming urban reforestation strategies.

Hopefully, this study will raise the attention of scientists and policymakers working in the field of urban and peri-urban reforestation, as well as those working on ESs modeling. Even though high-resolution multispectral satellite imagery is widely used when it comes to assessing vegetation's structural parameters, processes, and ESs delivery (García-Pardo et al. 2022), one must take into account that (1) Sentinel-2 and Landsat 8 LAI estimates may have moderate accuracy and precision, and (2) at the peak of the vegetative growth, SIs saturation is

likely to occur for densely vegetated areas. In such conditions, satellite-derived LAI estimates, and consequently, ESs estimates, are susceptible to a certain degree of underestimation.

Our study presents some general limitations that should be properly identified and addressed in upcoming works. It was entirely conducted during the early summer of 2021; therefore, a multi-seasonal assessment of the relationship between satellite-derived spectral indices and the field-measured LAI is needed to provide more comprehensive results. Indeed, factors such as phenology, cold stress, and soil moisture are likely to deeply influence such a relation.

Spectrum saturation, especially when it comes to estimating the LAI, is a well-known limitation (Wang et al. 2022), which also affected our study.

The use of LI-COR LAI 2200c also shows some considerable flaws. For example, LI-COR LAI 2200c relies on several assumptions (e.g., leaves do not transmit nor reflect incident radiation; leaves are randomly distributed; leaves show a random azimuthal distribution) which are rarely concurrently satisfied by any canopy (Danner et al. 2015). Besides such assumptions, the quality of measures is also influenced by factors such as the evenness of sky lighting and camera positioning (Lenz et al. 1997; Jonckheere et al. 2004), which we controlled by (1) making measures during cloud-free days; (2) exposing the camera parallel to the ground, and (3) applying the scattering correction implemented in the FV2200 software.

Despite the marked forest management (e.g., thinning and removal of dead wood), the PECp can still be considered a natural forest, due to its remarkable size and presence of autochthonous species; therefore, our results might not apply to small parks, which often also host alien species.

Lastly, even though the forest's understory was very sparse, its impact should be accounted for in both direct LAI measurements and remote sensing-based estimates (George et al. 2021).

Conclusions

In this study, we tested the performance of two widely used high-resolution multispectral sensors, that is, Sentinel-2 and Landsat 8, in estimating the summer leaf area index in a Mediterranean peri-urban forest. To do so, we performed a single linear regression between 10 spectral indices and 193 field LAI measurements, collected for different functional groups of vegetation.

We found that Landsat 8-derived models have, on average, a slightly better performance, with the best model (the one based on NDVI) showing an R^2 of 0.55 and NRMSE of 14.74%, compared to R^2 of 0.52 and NRMSE of 15.15% showed by the best Sentinel-2 model, which is based on the NBR. However, both sensors showed moderate performances in estimating the LAI. In general, 30-m and 20-m resolution models outperformed the 10-m resolution ones. All models were affected by spectrum saturation: as a result, we do not recommend estimating high LAI values (above 5) using a remote sensing-based approach.

It is noteworthy that the satellite-derived LAI is often used as a key input parameter for assessing numerous ESs, which in turn play a pivotal role in the enhancement of human health and well-being and are rising as a key feature steering new urban forestation strategies (Manes et al. 2016). Therefore, the uncertainty introduced using satellite-derived LAI in such estimates should be accounted for.

Acknowledgements
Not applicable.

Author contributions
FM designed and supervised the study; RS provided the Li-COR LAI-2200c. AS conducted the field campaign, made the remote sensing and statistical elaborations, and wrote the main draft of the manuscript. AS, FM and RS critically reviewed the manuscript at various stages and interpreted the data.

Funding
Progetto: Servizi Ecosistemici e Infrastrutture Verdi urbane e peri-urbane nell'area Metropolitana Romana: stima del contributo delle foreste naturali di Castelporziano nel miglioramento della qualità dell'aria della città di Roma. Accademia Nazionale delle Scienze detta dei XL, in collaborazione con Segretariato Generale della Presidenza della Repubblica. PRO-ICOS_MED Potenziamento della Rete di Osservazione ICOS-Italia nel Mediterraneo—Rafforzamento del capitale umano" funded by the Ministry of Research. PNRR, Missione 4, Componente 2, Avviso 3264/2021, IR0000032—ITINERIS—Italian Integrated Environmental Research Infrastructures System CUP B53C22002150006. The funding bodies equally contributed to the various steps of this study.

Availability of data and materials
The datasets used and/or analyzed during the current study are available from the corresponding author on reasonable request.

Declarations

Ethics approval and consent to participate
Not applicable.

Consent for publication
Not applicable.

Competing interests
Authors declare they have no competing interests.

Author details
[1] Research Centre for Forestry and Wood (FL), Council for Agricultural Research and Economics (CREA), Via Valle Della Quistione 27, 00166 Rome, Italy. [2]Research Institute On Terrestrial Ecosystems (IRET), National Research Council of Italy (CNR), Strada Provinciale 35d, 9, 00015 Monterotondo (RM), Italy. [3]Presidential Estate of Castelporziano, Via Pontina 690, 00128 Rome, Italy. [4]Department of Environmental Biology, Sapienza University of Rome, P.Le Aldo Moro, 5, 00185 Rome, Italy.

Received: 25 February 2023 Accepted: 5 June 2023
Published online: 14 June 2023

References

Aklilu Tesfaye A, Gessesse Awoke B (2021) Evaluation of the saturation property of vegetation indices derived from Sentinel-2 in mixed crop-forest ecosystem. Spat Inf Res 29:109–121. https://doi.org/10.1007/s41324-020-00339-5

Anselmi S, Chiesi M, Giannini M, Manes F, Maselli F (2004) Estimation of Mediterranean forest transpiration and photosynthesis through the use of an ecosystem simulation model driven by remotely sensed data: simulation of Mediterranean forest functional processes. Glob Ecol Biogeogr 13:371–380. https://doi.org/10.1111/j.1466-822X.2004.00101.x

Bagnouls F (1953) Saison sèche et indice xérothermique. Faculté des Sciences. 8. Revue De Géographie De Lyon 29(3):269

Bazzanti M (2015) Pond macroinvertebrates of the Presidential Estate of Castelporziano (Rome): a review of ecological aspects and selecting indicator taxa for conservation. Rend Fis Acc Lincei 26:337–343. https://doi.org/10.1007/s12210-015-0431-4

Blasi C, Capotorti G, Alós Ortí MM, Anzellotti I, Attorre F, Azzella MM, Carli E, Copiz R, Garfì V, Manes F, Marando F, Marchetti M, Mollo B, Zavattero L (2017) Ecosystem mapping for the implementation of the European Biodiversity Strategy at the national level: the case of Italy. Environ Sci Policy 78:173–184. https://doi.org/10.1016/j.envsci.2017.09.002

Breda NJJ (2003) Ground-based measurements of leaf area index: a review of methods, instruments and current controversies. J Exp Bot 54:2403–2417. https://doi.org/10.1093/jxb/erg263

Bréda NJJ (2008) Leaf area index. In: Encyclopedia of Ecology. Elsevier, pp 457–462. https://doi.org/10.1016/B978-0-444-63768-0.00849-0

Brown LA, Fernandes R, Djamai N, Meier C, Gobron N, Morris H, Canisius F, Bai G, Lerebourg C, Lanconelli C, Clerici M, Dash J (2021) Validation of baseline and modified Sentinel-2 Level 2 Prototype Processor leaf area index retrievals over the United States. ISPRS J Photogramm Remote Sens 175:71–87. https://doi.org/10.1016/j.isprsjprs.2021.02.020

Castracani C, Grasso DA, Fanfani A, Mori A (2010) The ant fauna of Castelporziano Presidential Reserve (Rome, Italy) as a model for the analysis of ant community structure in relation to environmental variation in Mediterranean ecosystems. J Insect Conserv 14:585–594. https://doi.org/10.1007/s10841-010-9285-3

Chrysafis I, Korakis G, Kyriazopoulos AP, Mallinis G (2020) Retrieval of leaf area index using sentinel-2 imagery in a mixed Mediterranean forest area. ISPRS Int J Geo-Inf 9:622. https://doi.org/10.3390/ijgi9110622

Clevers JGPW, Gitelson AA (2013) Remote estimation of crop and grass chlorophyll and nitrogen content using red-edge bands on Sentinel-2 and -3. Int J Appl Earth Obs Geoinf 23:344–351. https://doi.org/10.1016/j.jag.2012.10.008

Congedo L (2016) Semi-Automatic Classification Plugin Documentation. Release 6.0.1.1. https://doi.org/10.13140/RG.2.2.29474.02242/1

Conte A, Zappitelli I, Fusaro L, Alivernini A, Moretti V, Sorgi T, Recanatesi F, Fares S (2022) Significant loss of ecosystem services by environmental changes in the Mediterranean coastal area. Forests 13:689. https://doi.org/10.3390/f13050689

Costanza R, de Groot R, Sutton P, van der Ploeg S, Anderson SJ, Kubiszewski I, Farber S, Turner RK (2014) Changes in the global value of ecosystem services. Glob Environ Chang 26:152–158. https://doi.org/10.1016/j.gloenvcha.2014.04.002

Cutini A, Matteucci G, Mugnozza GS (1998) Estimation of leaf area index with the Li-Cor LAI 2000 in deciduous forests. For Ecol Manage 105:55–65. https://doi.org/10.1016/S0378-1127(97)00269-7

Danner M, Locherer M, Hank T, Richter K (2015) Measuring Leaf Area Index (LAI) with the LI-Cor LAI 2200C or LAI-2200 (+2200Clear Kit)—theory, measurement, problems, interpretation. EnMAP Flight Campaigns Technical Report; https://doi.org/10.2312/ENMAP.2015.009

Deshayes M, Guyon D, Jeanjean H, Stach N, Jolly A, Hagolle O (2006) The contribution of remote sensing to the assessment of drought effects in forest ecosystems. Ann for Sci 63(6):579–595. https://doi.org/10.1051/forest:2006045

Di Sora N, Rossini L, Contarini M, Chiarot E, Speranza S (2022) Endotherapic treatment to control *Toumeyella parvicornis* Cockerell infestations on *Pinus pinea* L. Pest Manag Sci 78(6):2443–2448. https://doi.org/10.1002/ps.6876

Djamai N, Fernandes R (2018) Comparison of SNAP-derived sentinel-2A L2A product to ESA product over Europe. Remote Sens 10:926. https://doi.org/10.3390/rs10060926

Dong T, Liu J, Qian B, He L, Liu J, Wang R, Jing Q, Champagne C, McNairn H, Powers J, Shi Y, Chen JM, Shang J (2020) Estimating crop biomass using leaf area index derived from Landsat 8 and Sentinel-2 data. ISPRS J Photogramm Remote Sens 168:236–250. https://doi.org/10.1016/j.isprsjprs.2020.08.003

EC (2020a) EU Biodiversity Strategy for 2030—Bringing nature back into our lives. Accessed at https://www.eea.europa.eu/policy-documents/eu-biodiversity-strategy-for-2030-1 on October 2022

EC (2020b). Proposal for a Regulation of the European Parliament and of the Council on nature restoration. EU Biodiversity Strategy for 2030—Bringing nature back into our lives. Accessed at https://www.eea.europa.eu/policy-documents/eu-biodiversity-strategy-for-2030-1 on October 2022

European Commission (EC) (2022) Proposal for a regulation of the European Parliament and of the Council on nature restoration. Brussels, 22.6.2022. COM(2022) 304 final. 2022/0195 (COD). Accessed at https://environment.ec.europa.eu/system/files/2022-06/Proposal%20for%20a%20Regulation%20on%20nature%20restoration.pdf on May 2023

Enssle F, Kabisch N (2020) Urban green spaces for the social interaction, health and well-being of older people—an integrated view of urban ecosystem services and socio-environmental justice. Environ Sci Policy 109:36–44. https://doi.org/10.1016/j.envsci.2020.04.008

EOS data analytics (2022) NDMI (Normalized Difference Moisture Index). Accessed at https://eos.com/make-an-analysis/ndmi/#:~:text=The%20NDMI%20range%20is%20%2D1,NDMI%20values%20could%20signal%20waterlogging on December 2022

ESA (2023) Sentinel online overview. Accessed at https://sentinels.copernicus.eu/web/sentinel/missions/sentinel-2/overview on October 2022

Farrugia S, Hudson MD, McCulloch L (2013) An evaluation of flood control and urban cooling ecosystem services delivered by urban green infrastructure. Int J Biodiversity Sci Ecosyst Serv Manag 9:136–145. https://doi.org/10.1080/21513732.2013.782342

Filipponi F (2021) Comparison of LAI estimates from high resolution satellite observations using different biophysical processors. In: IECAG 2021. Presented at the IECAG 2021, MDPI, p 5. https://doi.org/10.3390/IECAG2021-09683

Fuster B, Sánchez-Zapero J, Camacho F, García-Santos V, Verger A, Lacaze R, Weiss M, Baret F, Smets B (2020) Quality assessment of PROBA-V LAI, fAPAR and fCOVER collection 300 m products of copernicus global land service. Remote Sens 12:1017. https://doi.org/10.3390/rs12061017

Galmés J, Medrano H, Flexas J (2007) Photosynthetic limitations in response to water stress and recovery in Mediterranean plants with different growth forms. New Phytol 175(1):81–93. https://doi.org/10.1111/j.1469-8137.2007.02087.x

Gao X (2000) Optical-biophysical relationships of vegetation spectra without background contamination. Remote Sens Environ 74:609–620. https://doi.org/10.1016/S0034-4257(00)00150-4

García-Pardo KA, Moreno-Rangel D, Domínguez-Amarillo S, García-Chávez JR (2022) Remote sensing for the assessment of ecosystem services provided by urban vegetation: a review of the methods applied. Urban For Urban Green 74:127636. https://doi.org/10.1016/j.ufug.2022.127636

George J-P, Yang W, Kobayashi H, Biermann T, Carrara A, Cremonese E, Cuntz M, Fares S, Gerosa G, Grünwald T, Hase N, Heliasz M, Ibrom A, Knohl A, Kruijt B, Lange H, Limousin J-M, Loustau D, Lukeš P, Marzuoli R, Mölder M, Montagnani L, Neirynck J, Peichl M, Rebmann C, Schmidt M, Serrano FRL, Soudani K, Vincke C, Pisek J (2021) Method comparison of indirect assessments of understory leaf area index (LAIu): a case study across the extended network of ICOS forest ecosystem sites in Europe. Ecol Indicators 128:107841. https://doi.org/10.1016/j.ecolind.2021.107841

Gronau QF, Wagenmakers E-J (2019) Limitations of Bayesian leave-one-out cross-validation for model selection. Comput Brain Behav 2:1–11. https://doi.org/10.1007/s42113-018-0011-7

Guijarro JA (2019) climatol: Climate Tools (Series Homogenization and Derived Products)

Hoff C, Rambal S (2003) An examination of the interaction between climate, soil and leaf area index in a *Quercus ilex* ecosystem. Ann For Sci 60(2):153–161. https://doi.org/10.1051/forest:2003008

Jiang B, Liang S, Wang J, Xiao Z (2010) Modeling MODIS LAI time series using three statistical methods. Remote Sens Environ 114:1432–1444. https://doi.org/10.1016/j.rse.2010.01.026

Jonckheere I, Fleck S, Nackaerts K, Muys B, Coppin P, Weiss M, Baret F (2004) Review of methods for in situ leaf area index determination: Part I. Theories, sensors and hemispherical photography. Agric For Meteorol 121(1–2):19–35. https://doi.org/10.1016/j.agrformet.2003.08.027

Kosanic A, Petzold J (2020) A systematic review of cultural ecosystem services and human wellbeing. Ecosyst Serv 45:101168. https://doi.org/10.1016/j.ecoser.2020.101168

Kuhn M, Wing J, Weston S, Williams A (2022) caret: Classification and Regression Training. Accessed at https://cran.r-project.org/package=caret on October 2022

Langemeyer J, Connolly JJT (2020) Weaving notions of justice into urban ecosystem services research and practice. Environ Sci Policy 109:1–14. https://doi.org/10.1016/j.envsci.2020.03.021

Lausi L, Amodio M, Sebastiani A, Fusaro A, Manes F (2022) Assessing cultural ecosystem services during the Covid-19 pandemic at the Garden of Ninfa (Italy). Annali Di Botanica 12:63–75. https://doi.org/10.13133/2239-3129/17681

Lenz R, Selige T, Seufert G (1997) Scaling up the biogenic emissions from test sites at Castelporziano. Atmos Environ 31:239–250. https://doi.org/10.1016/S1352-2310(97)00267-7

Leviston Z, Walker I, Green M, Price J (2018) Linkages between ecosystem services and human wellbeing: a Nexus Webs approach. Ecol Indic 93:658–668. https://doi.org/10.1016/j.ecolind.2018.05.052

LI-COR Biosciences (2013) LAI-2200 Plant Canopy Analyzer instruction manual. Accessed at https://www.licor.com/env/support/LAI-2200C/manuals.html on June 2021

Louis J, Debaecker V, Pflug B, Main-Knorn M, Bieniarz J, Mueller-Wilm U, Cadau E, Gascon F (2016) sentinel-2 sen2cor: l2a processor for users 8. Proc. 'Living Planet Symposium 2016', Prague, Czech Republic, 9–13 May 2016 (ESA SP-740, August 2016)

Manes F, Anselmi S, Canfora E, Giannini M (1997a) Remote sensing analysis of Mediterranean ecosystem canopies and upscaling studies. In: Cecchi G, Engman ET, Zilioli E (eds) Presented at the Aerospace Remote Sensing '97, London, United Kingdom, pp 246–252. https://doi.org/10.1117/12.298133

Manes F, Grignetti A, Tinelli A, Lenz R, Ciccioli P (1997b) General features of the Castelporziano test site. Atmos Environ 31:19–25. https://doi.org/10.1016/S1352-2310(97)00070-8

Manes F, Astorino G, Vitale M, Loreto F (1997c) Morpho-functional characteristics of *Quercus ilex* L. leaves of different age and their ecophysiological behaviour during different seasons. Plant Biosyst 131:149–158. https://doi.org/10.1080/11263504.1997.10654176

Manes F, Seufert G, Vitale M (1997d) Ecophysiological studies of Mediterranean plant species at the Castelporziano estate. Atmos Environ 31:51–60. https://doi.org/10.1016/S1352-2310(97)00073-3

Manes F, Incerti G, Salvatori E, Vitale M, Ricotta C, Costanza R (2012) Urban ecosystem services: tree diversity and stability of tropospheric ozone removal. Ecol Appl 22:349–360. https://doi.org/10.1890/11-0561.1

Manes F, Silli V, Salvatori E, Incerti G, Galante G, Fusaro L, Perrino C (2014) Urban ecosystem services: tree diversity and stability of PM_{10} removal in the metropolitan area of Rome. Annali Di Botanica 4:19–26

Manes F, Marando F, Capotorti G, Blasi C, Salvatori E, Fusaro L, Ciancarella L, Mircea M, Marchetti M, Chirici G, Munafò M (2016) Regulating Ecosystem Services of forests in ten Italian Metropolitan Cities: air quality improvement by PM_{10} and O_3 removal. Ecol Indic 67:425–440. https://doi.org/10.1016/j.ecolind.2016.03.009

Manes F, Sebastiani A, Fusaro L, Salvatori E (2021) Servizi Ecosistemici di regolazione forniti dalle foreste periurbane e urbane nel territorio della Tenuta Presidenziale di Castelporziano: analisi di stress biotici e abiotici. "Il Sistema Ambientale della Tenuta presidenziale di Castelporziano. Ricerche sulla complessità di un ecosistema forestale costiero mediterraneo", Scritti e documenti LXII Accademia Nazionale delle Scienze detta dei XL, in collaborazione con Segretariato Generale della Presidenza della Repubblica

Marando F, Salvatori E, Sebastiani A, Fusaro L, Manes F (2019) Regulating Ecosystem Services and Green Infrastructure: assessment of Urban Heat Island effect mitigation in the municipality of Rome, Italy. Ecol Model 392:92–102. https://doi.org/10.1016/j.ecolmodel.2018.11.011

Meyer LH, Heurich M, Beudert B, Premier J, Pflugmacher D (2019) Comparison of Landsat-8 and Sentinel-2 data for estimation of leaf area index in temperate forests. Remote Sens 11:1160. https://doi.org/10.3390/rs11101160

Muresan AN, Sebastiani A, Gaglio M, Fano EA, Manes F (2022) Assessment of air pollutants removal by green infrastructure and urban and peri-urban forests management for a greening plan in the Municipality of Ferrara (Po river plain, Italy). Ecol Indic 135:108554. https://doi.org/10.1016/j.ecolind.2022.108554

Nardella L, Sebastiani A, Stafoggia M, Franzese PP, Manes F (2023) Modelling PM_{10} removal in three Italian coastal Metropolitan Cities along a latitudinal gradient. Ecol Model 483:110423. https://doi.org/10.1016/j.ecolmodel.2023.110423

Nowak DJ, McHale PJ, Ibarra M, Crane D, Stevens JC, Luley CJ (1998) Modeling the effects of urban vegetation on air pollution. In: Gryning S-E, Chaumerliac N (eds) Air pollution modeling and its application XII. Springer US, Boston, pp 399–407. https://doi.org/10.1007/978-1-4757-9128-0_41

Orioli R, Antonucci C, Scortichini M, Cerza F, Marando F, Ancona C, Manes F, Davoli M, Michelozzi P, Forastiere F, Cesaroni G (2019) Exposure to residential greenness as a predictor of cause-specific mortality and stroke incidence in the Rome longitudinal study. Environ Health Perspect 127:027002. https://doi.org/10.1289/EHP2854

Pasqualotto N, Delegido J, Van Wittenberghe S, Rinaldi M, Moreno J (2019) Multi-crop green LAI estimation with a new simple Sentinel-2 LAI Index (SeLI). Sensors 19:904. https://doi.org/10.3390/s19040904

Peng Y, Gitelson AA (2011) Application of chlorophyll-related vegetation indices for remote estimation of maize productivity. Agric For Meteorol 151:1267–1276. https://doi.org/10.1016/j.agrformet.2011.05.005

Reader R, Radford JS, Lieth H (1974) Modeling important phytophenological events in eastern North America. In: Phenology and seasonality modeling. pp 329–342. https://doi.org/10.1007/978-3-642-51863-8_27

Robinson SL, Lundholm JT (2012) Ecosystem services provided by urban spontaneous vegetation. Urban Ecosyst 15:545–557. https://doi.org/10.1007/s11252-012-0225-8

Sebastiani A, Fares S (2023) Spatial prioritization of ecosystem services for land conservation: the case study of central Italy. Forests 14:145. https://doi.org/10.3390/f14010145

Sebastiani A, Marando F, Manes F (2021a) Mismatch of regulating ecosystem services for sustainable urban planning: PM_{10} removal and urban heat island effect mitigation in the municipality of Rome (Italy). Urban For Urban Green 57:126938. https://doi.org/10.1016/j.ufug.2020.126938

Sebastiani A, Buonocore E, Franzese PP, Riccio A, Chianese E, Nardella L, Manes F (2021b) Modeling air quality regulation by green infrastructure in a Mediterranean coastal urban area: The removal of PM_{10} in the Metropolitan City of Naples (Italy). Ecol Model 440:109383. https://doi.org/10.1016/j.ecolmodel.2020.109383

Serbin SP, Ahl DE, Gower ST (2013) Spatial and temporal validation of the MODIS LAI and FPAR products across a boreal forest wildfire chronosequence. Remote Sens Environ 133:71–84. https://doi.org/10.1016/j.rse.2013.01.022

Seufert G, Bartzis J, Bomboi T, Ciccioli P, Cieslik S, Dlugi R, Foster P, Hewitt CN, Kesselmeier J, Kotzias D, Lenz R, Manes F, Pastor RP, Steinbrecher R, Torres L, Valentini R, Versino B (1997) An overview of the Castelporziano experiments. Atmos Environ 31:5–17. https://doi.org/10.1016/S1352-2310(97)00334-8

Sun Y, Qin Q, Ren H, Zhang T, Chen S (2020) Red-edge band vegetation indices for leaf area index estimation from sentinel-2/MSI imagery. IEEE Trans Geosci Remote Sens 58:826–840

Tesemma ZK, Wei Y, Peel MC, Western AW (2015) The effect of year-to-year variability of leaf area index on Variable Infiltration Capacity model performance and simulation of runoff. Adv Water Resour 83:310–322. https://doi.org/10.1016/j.advwatres.2015.07.002

Todd SW, Hoffer RM, Milchunas DG (1998) Biomass estimation on grazed and ungrazed rangelands using spectral indices. Int J Remote Sens 19:427–438. https://doi.org/10.1080/014311698216071

Vázquez-González C, Moreno-Casasola P, Peralta Peláez LA, Monroy R, Espejel I (2019) The value of coastal wetland flood prevention lost to urbanization on the coastal plain of the Gulf of Mexico: an analysis of flood damage

by hurricane impacts. Int J Disaster Risk Reduction 37:101180. https://doi.org/10.1016/j.ijdrr.2019.101180
Viña A, Gitelson AA, Nguy-Robertson AL, Peng Y (2011) Comparison of different vegetation indices for the remote assessment of green leaf area index of crops. Remote Sens Environ 115:3468–3478. https://doi.org/10.1016/j.rse.2011.08.010
Wang Q, Putri NA, Gan Y, Song G (2022) Combining both spectral and textural indices for alleviating saturation problem in forest LAI estimation using Sentinel-2 data. Geocarto Int 37:10511–10531. https://doi.org/10.1080/10106049.2022.2037730
Wong T-T (2015) Performance evaluation of classification algorithms by k-fold and leave-one-out cross validation. Pattern Recogn 48:2839–2846. https://doi.org/10.1016/j.patcog.2015.03.009
Xiao XD, Dong L, Yan H, Yang N, Xiong Y (2018) The influence of the spatial characteristics of urban green space on the urban heat island effect in Suzhou Industrial Park. Sustain Cities Soc 40:428–439. https://doi.org/10.1016/j.scs.2018.04.002
Yan K, Park T, Yan G, Liu Z, Yang B, Chen C, Nemani R, Knyazikhin Y, Myneni R (2016) Evaluation of MODIS LAI/FPAR product collection 6. Part 2: validation and intercomparison. Remote Sens 8:460. https://doi.org/10.3390/rs8060460
Zhou J, Yan Guo R, Sun M, Di TT, Wang S, Zhai J, Zhao Z (2017) The effects of GLCM parameters on LAI estimation using texture values from Quickbird Satellite Imagery. Sci Rep 7:7366. https://doi.org/10.1038/s41598-017-07951-w

Publisher's Note